Journal of Structural Geology 32 (2010) 216–221

Contents lists available at ScienceDirect

Journal of Structural Geology

journal homepage: www.elsevier.com/locate/jsg

Rb–Sr systematics of fault gouges from the North Anatolian Fault Zone (Turkey)

Halim Mutlu [a,*], I. Tonguç Uysal [b], Erhan Altunel [a], Volkan Karabacak [a], Yuexing Feng [c], Jian-xin Zhao [c], Ozan Atalay [a]

[a] Department of Geological Engineering, Eskişehir Osmangazi University, Eskişehir 26480, Turkey
[b] Queensland Geothermal Energy Centre of Excellence, The University of Queensland, Queensland 4072, Australia
[c] Radiogenic Isotope Facility, Centre for Microscopy and Microanalysis, The University of Queensland, Queensland 4072, Australia

ARTICLE INFO

Article history:
Received 2 April 2009
Received in revised form
13 November 2009
Accepted 18 November 2009
Available online 24 November 2009

Keywords:
North Anatolian Fault Zone
Fault gouge
Illitic clays
Rb–Sr dating

ABSTRACT

A combined mineralogical and Rb–Sr isotopic investigation was conducted on fault gouges from two locations at eastern part of the North Anatolian Fault Zone (NAFZ). The fault gouge samples contain no 2 M mica and consist chiefly of cryptocrystalline material, which is extensively altered to illitic clays (mixed-layered illite–smectite) and some carbonate minerals. The Rb–Sr isochrones of leachate, residue and untreated aliquots from various size fractions of samples yielded two different illite generations. The oldest illite authigenesis, which started at about 35.6 Ma might be inherited from pre-existing faults along the Tethyan suture zone. The authigenic illites from finer fractions correspond to an isochron age of 8.3 Ma, which is in agreement with the findings of previous works that may suggest a middle Miocene age for the initiation of the NAFZ. Our Sr isotope data indicate that the metamorphic fluids contain some mantle components and mobilised during fault movement.

1. Introduction

Dating of fault reactivations along active plate boundaries is important to understand the evolution of tectonic plate movements and interactions; however, radiometric dating of shallow crustal faulting remains highly challenging. In active tectonic zones, we can only use low temperature K-bearing authigenic minerals for age dating, which precipitate during surface or near-surface faulting in the crust's brittle regime. Complete syntectonic crystallisation and isotopic homogenisation is, however, generally not achieved in low temperature shallow environments. Thus illitic clay minerals separated from fault gouges are composed of a mixture of authigenic 1 M illite formed during faulting and detrital 2 M illite inherited from the host rock. Recently, a number of studies have demonstrated that such clays can be dated successfully by plotting percentage detrital 2 M illite against the K–Ar or Ar–Ar dates of the clays with a range of size fractions (e.g., from <0.2 to 2–1) that allow extrapolation to apparent ages for detrital and authigenic end members (Grathoff et al., 2001; van der Pluijm et al., 2001, 2006; Haines and van der Pluijm, 2008). Similarly, using K–Ar analysis of various illite size fractions combined with X-ray diffraction quantification of detrital and authigenic endmembers we determined the age of syntectonic illite generation in a fault gouge from the central part of a plate boundary strike-slip fault system, the North Anatolian Fault Zone (NAFZ) in Turkey (Fig. 1A–B) (Uysal et al., 2006). Our finding suggests that significant strike-slip fault movements initiated at ~57 Ma, immediately after the continental collision related to the closure of the Neotethys Ocean. On eastern segments of the NAFZ, clay minerals were formed through syntectonic hydrothermal alteration of fault gouges containing pseudotachylyte bands, and no detrital contaminations are present in such samples (Uysal et al., 2006). Intense hydrothermal alteration gave rise to complete recrystallisation of detrital phyllosilicate phases with precipitation of mixed-layered illite–smectite. Although such clays represent a pure authigenic mineral population, their radiometric age dating is also not straightforward. In active fault systems, newly formed illitic clays are subjected to episodic heat and fluid flow events. Heating of earlier formed authigenic illitic clays during fault reactivation to a temperature close to or above their crystallisation temperature causes partly or completely resetting of their isotopic systematics (Clauer and Chaudhuri, 1999). Mixed-layered illite–smectite as a common authigenic clay phase in fault gouges is particularly susceptible to younger thermal events because of their very small crystal sizes and hence their higher surface area to volume ratios. As a result, such clays can experience redissolution and recrystallisation a number of times during the evolution of the fault activity and thus yield decreasing K–Ar dates with decreasing grain sizes.

* Corresponding author. Tel.: +90 222 239 3750; fax: +90 222 229 0535.
E-mail address: hmutlu@ogu.edu.tr (H. Mutlu).

0191-8141/$ – see front matter © 2009 Elsevier Ltd. All rights reserved.
doi:10.1016/j.jsg.2009.11.006

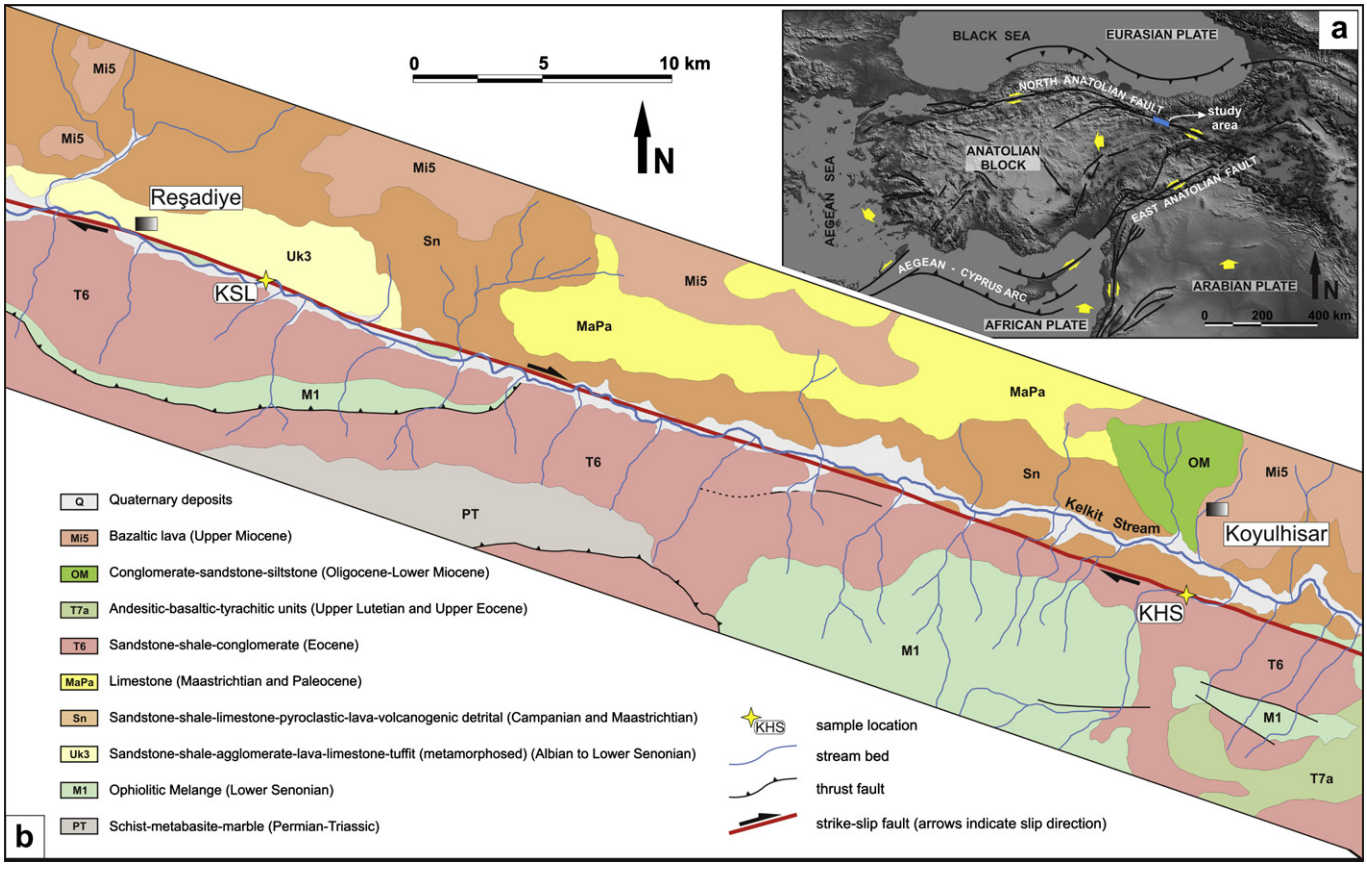

Fig. 1. (A) Simplified Neotectonic setting of Turkey (modified from McClusky et al., 2000; Bozkurt, 2001). (B) Geological and location map of the investigated areas (modified from Herece and Akay, 2003).

Consequently, reliable interpretation of such age data as mixed ages due to incomplete isotopic resetting or real crystallisation ages related to episodic fault activations is difficult. For example, inclined K–Ar age spectra relative to clay particle size from fault gouges in the eastern part of the NAFZ indicate that displacements along the NAFZ have taken place continuously following the initiation of the fault movements in the latest Paleocene–Early Eocene (Uysal et al., 2006), so that the timing of significant individual fault reactivation episodes remains unknown.

The Rb–Sr isotope system has been extensively used in geochronological studies of illite authigenesis in mudrocks and sandstones (Gilg and Frei, 1994; Clauer and Chaudhuri, 1995; Uysal et al., 2001). Three point isochrones constructed from the untreated, acid-leached residue and leachate samples have been used to evaluate the extent of Rb–Sr isotopic homogenisation and date the illite authigenesis in sedimentary basins (Clauer et al., 1993; Clauer and Chaudhuri, 1995). In the current paper, we show that the Rb–Sr isotopic system can also be used to evaluate the degree of isotopic homogenisation and determine the timing of syntectonic illite–smectite precipitation in near-surface fault gouges. Our results also add insight into the reactivation history of the North Anatolian Fault Zone, which is critical in understanding the plate tectonic evolution of the eastern Mediterranean region (e.g., Şengör and Yilmaz, 1981; Okay et al., 2008).

2. Sample locations and description

Location KSL is situated near the town Reşadiye within a crushed zone in the Eocene sandstone-shale unit (Fig. 1B). The sandstone-shale unit exposed outside the fault zone represents the undeformed parent rock. The phyllosilicate mineral phase in the parent rocks consists of mainly chlorite with some mica, which are absent in the KSL fault rocks. The fault gouge samples consist of isotropic, glassy or cryptocrystalline groundmass (pseudotachylyte) interlayered with quartz-rich fine-grained clastic material. The glassy or cryptocrystalline material is significantly altered to illitic clays, kaolinite, and ankerite–calcite carbonate association (see Uysal et al., 2006 for more information).

Fig. 2. Thin section image of sample KHS showing glassy or cryptocrystalline material associated with emplacement of microscopic carbonate (ankerite–calcite) veins.

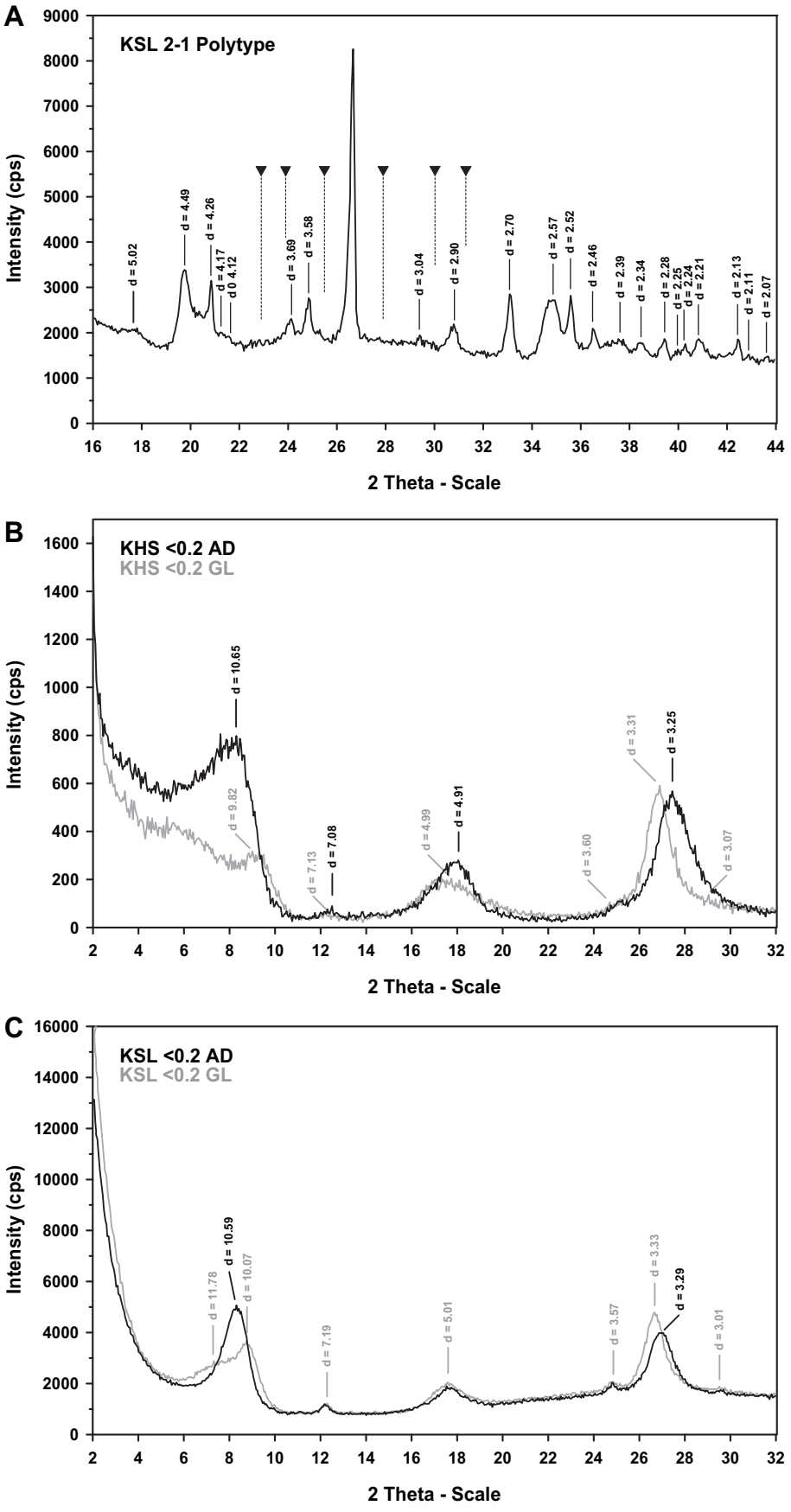

Fig. 3. X-ray diffraction tracings of fault gouge samples. (A) The random powder 2–1 μm fraction of sample KSL (diagnostic peaks of 2 M illite polytype (triangles) are from Grathoff and Moore (1996)); (B) Air-dried (AD) and glycolated (GL) scan for <0.2 μm fraction of sample KHS (note the shift of the 10.7-Å peak towards the high angle area with ethylene glycolation); (C) Air-dried (AD) and glycolated (GL) scan for <0.2 μm fraction of sample KSL (note an asymmetrical peak at ~10 Å, with a broad shoulder when glycolated).

Location KHS is situated on a road cut between the towns of Reşadiye and Koyulhisar within a deformed peridotite in the Cretaceous ophiolitic mélange. Phyllosilicate alteration minerals in the peridotite parent rock consist of only kaolinite and chlorite. The fault gouge material occurs as injected vein fillings along fractures of up to 30 cm in thickness and 5–6 m long (Fig. 2). Similar to the samples in location KSL, the fault gouge contains thin pseudotachylyte veins and interlayered quartz-rich material. Intense hydrothermal alteration was responsible for illitization of glassy or cryptocrystalline material, which is associated with emplacement of microscopic carbonate (ankerite–calcite) veins.

According to random powder XRD analysis, even the coarsest clay size fractions (2–1 μm) of the fault gouge samples contain no 2 M mica (Fig. 3A). The <0.2 μm fraction of the fault gouge samples in KHS and KSL locations consists of almost pure mixed-layered illite–smectite (Fig. 3B–C).

3. Tectonic and geological setting

The closure of the Neotethyan Ocean marks the beginning of Neotectonic period in Turkey. The convergence between the African and Eurasian plates in the late Cretaceous and the Arabian plate in Miocene resulted in placement of huge ophiolite nappes along the Izmir-Ankara-Erzincan Suture in northern Turkey. The demise of convergence was followed by a compressional-extensional tectonic regime in the Miocene that caused development of North Anatolian Fault Zone (NAFZ) along which the Anatolian block moves westwards (Şengör and Yilmaz, 1981) (Fig. 1A).

Previous studies suggest that the NAFZ is a regionally important right-lateral transform zone between the Eurasian plate and the Anatolian block (e.g. Bozkurt, 2001) (Fig. 1A). This zone is characterised by numerous fault segments, which are typically parallel to the plate motion. The WNW-ESE trending Reşadiye–Koyulhisar fault represents one of the segments on the NAFZ (Fig. 1B). Geological and geomorphological field data document prominent evidence for the right-lateral faulting. The fault extends in an N70–75W direction and has a simple strike-slip geometry characterised by nearly vertical fault planes and horizontal slickenside between Reşadiye in west and Koyulhisar in the east. The Kelkit Stream follows linear deformation zone through the fault.

4. Analytical methods

The XRD analyses were carried out on an X-ray diffractometer equipped with parallel beam geometry and CuKα radiation, operated at 40 kV and 40 mA at a scanning rate of 1°2θ/min. The samples were prepared for separation of the clay fraction by gently crushing the rocks to sand size, followed by disaggregation in distilled water using an ultrasonic bath. Different clay size fractions were obtained by centrifuging, and the decanted suspensions were placed on a glass slide. Following XRD analysis of air-dried samples, the oriented clay-aggregate mounts were placed in an ethylene–glycol atmosphere at 30–40 °C overnight prior to additional XRD analyses. Some random powder samples were scanned from 16 to 44°2θ in the step-scanning mode with a step size of 0.05° and a counting time of 30 s per step.

For the Rb–Sr dating, illitic clay separates were leached for 15 min at room temperature in 1*N* distilled HCl (cf. Clauer et al., 1993). Leachate and residue were separated by centrifuging. The residue was rinsed repeatedly with deionised water, dried and reweighed. Leachate, residue and untreated samples were spiked with ^{85}Rb–^{84}Sr and dissolved in a mixture of distilled HF and HNO_3. The Sr-enriched fraction was separated using cation exchange resin. Sr isotopic ratios were measured on a VG Sector 54 thermal ionisation mass spectrometer at the University of Queensland. Sr isotopic ratios were corrected for mass discrimination using $^{86}Sr/^{88}Sr = 0.1194$. Long-term repeated analyses of the SRM 987 international standard yield a mean $^{87}Sr/^{86}Sr$ value of 0.710249 ± 0.000028 (2σ). External reproducibility for $^{87}Rb/^{86}Sr$ was estimated to be ~0.5%. Rb–Sr isochron ages were calculated using program ISOPLOT (Ludwig, 2003).

5. Results

Rb–Sr isotope analysis was conducted for the untreated, leachates, and acid-leached (residues) clay fractions from fault gouges from location KHS (on the Niksar – Erzincan section between the towns of Reşadiye and Koyulhisar) and location KSL (situated near the town Reşadiye on the Niksar – Erzincan section). We analysed the same clay size fractions as we did for the K–Ar analysis (see Uysal et al., 2006). In the current study, we also analysed 0.5–0.2 μm fraction for KHS and 0.2–0.1 μm and <0.1 μm fractions for KSL samples. The whole data are presented in Table 1 and plotted on Rb–Sr isochron diagrams in Figs. 4 and 5. The slope of the linear relationship between $^{87}Sr/^{86}Sr$ and $^{87}Rb/^{86}Sr$ ratios for leachate-residue-untreated fractions from the 0.5–0.2 μm size fraction, and leachate-untreated fractions from the <0.2 μm size fraction in location KHS corresponds to an age of 35.6 ± 1.9 Ma (2σ, MSWD = 9.8) (initial $^{87}Sr/^{86}Sr = 0.70554 \pm 0.00019$) (Fig. 4A). This Rb–Sr isochron age is consistent with the K–Ar date of <0.2 μm fraction from the fault gouge in the same location (Uysal et al., 2006; Table 1). Excluding data of the <0.2 μm size fraction yields a better defined linear relationship with an age of 35.6 ± 0.53 Ma (2σ, MSWD = 1.2) (initial $^{87}Sr/^{86}Sr = 0.705575 \pm 0.00005$) (Fig. 4B).

The Rb–Sr isotope data for 0.1–0.2 μm fraction of two untreated sub-samples at KSL location, and leachate-residue-untreated fractions from the <0.1 μm size fraction for the same samples show linear relationships corresponding to an age of 8.5 ± 1.2 Ma (2σ, MSWD = 5.8) (initial $^{87}Sr/^{86}Sr = 0.706103 \pm 0.00009$) (Fig. 5A). Plotting only leachate-residue-untreated fractions from the <0.1 μm size fraction results in less data scattering that gives an age of 8.30 ± 0.95 Ma (2σ, MSWD = 2.8) (initial $^{87}Sr/^{86}Sr = 0.706146 \pm 0.00008$) (Fig. 5B). The Rb–Sr isochron ages of <0.2 μm clay fractions from KSL location are in agreement with the K–Ar date of <0.2 μm fraction from the same fault gouge sample in this location (Uysal et al., 2006; Table 1). Leachate-residue-untreated fractions

Table 1
Rb–Sr data.

Sample	Rb (ppm)	Sr (ppm)	$^{87}Rb/^{87}Sr$	$^{87}Sr/^{86}Sr$	2 (%)
KSL > 4U	77.50	397.2	0.5644	0.706370	0.0014
KSL > 4R	99.25	168.7	1.702	0.706875	0.0012
KSL > 4L	46.24	695.6	0.1923	0.706123	0.0012
KSL-4-2U	108.1	413.6	0.7559	0.706266	0.0012
KSL-4-2R	122.8	205.5	1.729	0.706736	0.0014
KSL-4-2L	252.0	2732	0.2668	0.706186	0.0012
KSL-2-1U	129.9	467.0	0.8049	0.706433	0.0014
KSL-2-1R	152.0	236.6	1.859	0.706717	0.0014
KSL-2-1L			0.2637	0.706200	0.0014
KSL-A/0.1–0.2U	214.0	325.6	1.901	0.706241	0.0012
KSL-B/0.1–0.2U	223.5	427.3	1.513	0.706171	0.0038
KSL-A < 0.1L	30.05	5865	0.0148	0.706181	0.001
KSL-A < 0.1R	58.17	12.59	13.370	0.707768	0.001
KSL-A < 0.1U	213.3	1031	0.5987	0.706196	0.0012
KSL-B < 0.1L	43.11	7147	0.0174	0.706205	0.0016
KSL-B < 0.1R	230.73	95.15	7.015	0.706893	0.0016
KSL-B < 0.1U	200.37	1105	0.5246	0.706174	0.0016
KHS0.5-0.2U	144.63	328.6	1.273	0.706189	0.0014
KHS0.5-0.2R	148.04	25.89	16.57	0.713945	0.0012
KHS0.5-0.2L	621.58	6997	0.2570	0.705730	0.0012
KHS < 0.2U	151.06	300.1	1.456	0.706122	0.0014
KHS < 0.2L	2200	29 546	0.2154	0.705744	0.0014

U = untreated, R = residue, L = leacheate.

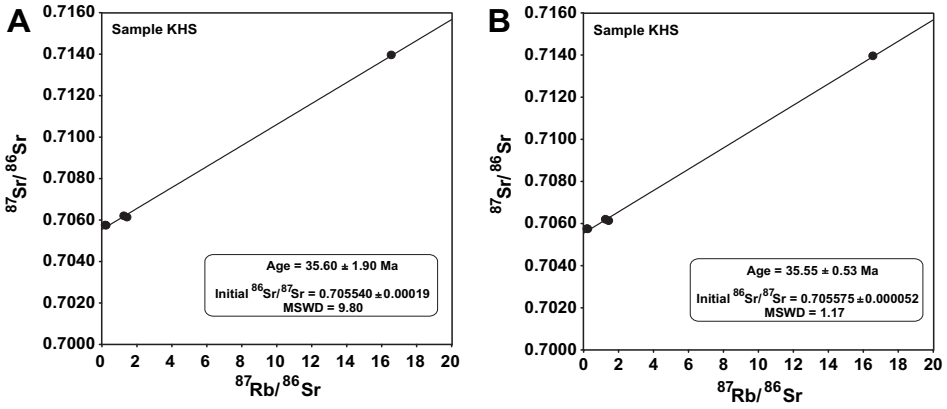

Fig. 4. Rb–Sr isochron diagrams for location KHS (A) The leachate-residue-untreated fractions from the 0.5–0.2 μm size fraction and leachate-untreated fractions from the <0.2 μm size fraction. (B) The leachate-residue-untreated fractions from the 0.5–0.2 μm size.

from 2 to 1 μm, 4 to 2 μm and >4 μm size fractions for KSL samples form a poorly developed linear array on the Rb–Sr diagram and yield a date with a large error of 27.5 ± 6.9 Ma (2σ, MSWD = 5.1) (initial $^{87}Sr/^{86}Sr = 0.70608 \pm 0.0001$) (Fig. 5C).

6. Discussion

6.1. Rb–Sr isotope system

Finest clay size separates of fault gouges in location KSL and KHS display well-developed linear data arrays on a Rb–Sr isochron diagram. Such linear relations can be a result of either a mixing between an older detrital illite population and a younger authigenic illite–smectite generation, or a complete isotopic equilibration of the entire authigenic clay separates at the same time. In the former case, the linear relationship between $^{87}Rb/^{86}Sr$ and $^{87}Sr/^{86}Sr$ would represent a mixing line of two end members with no meaningful age information, whereas the latter relation would provide an isochron whose slope yields the age of illitic clay generation during a fault reactivation event. X-ray diffraction patterns of random powder mounts of all clay size fractions from KSL and KHS samples show no characteristic peak positions of detrital 2 M illite (Uysal et al., 2006) (Fig. 3A). Detailed SEM and TEM analyses also confirm that the samples consist of entirely newly grown authigenic illite–smectite (see Fig. 2 in Uysal et al., 2006), and thus the linear relationships in Figs. 4 and 5 represent isochron ages of the syntectonic clay precipitations. The isochron ages are consistent with K–Ar dates of the same clay size fractions of the corresponding samples (Table 1) that provides a further support for meaningful age information.

The poorly developed linear array on the Rb–Sr diagram for >0.2 μm fractions of sample KSL can be attributed to disturbance of the original Rb–Sr isotopic system of during younger fault reactivation events. The thermal events associated with younger fault movements could lead to entire recrystallisation of only <0.5 μm and <0.2 μm fractions for KHS and KSL samples respectively, whereas the coarser clay components were partly recrystallised causing the scatter on the Rb–Sr diagram. Consequently, the timing of the initial hydrothermal event that was responsible for the initial alteration of parent rocks will remain unknown in KHS and KSL locations.

In addition to age information, Rb–Sr isochron diagram can also provide an insight into the Sr isotope composition of fluids from which illitic clays have precipitated. Acid leachable components of the clay fractions are derived mainly from coexisting fine-grained carbonate minerals. Ankerite and calcite are common authigenic phases that occur as microveins in fault gouges in KHS and KSL locations (Fig. 2). The well-developed isochron diagrams in Figs. 4 and 5 that consist of data points for leachates, residue and untreated clays indicate that Rb–Sr isotopic equilibrium was achieved between authigenic illite–smectite and carbonate mineral phases during faulting events. The unradiogenic initial $^{87}Sr/^{86}Sr$ ratio of 0.7055 for KHS samples is consistent with the rare earth element (REE) composition of these clays that indicates interaction of K-bearing deep fluids with Rb-poor primitive mantle-derived ophiolitic rocks (cf. Uysal et al., 2006). Likewise, the more radiogenic initial $^{87}Sr/^{86}Sr$ ratio of 0.7061 for KSL clays is in agreement

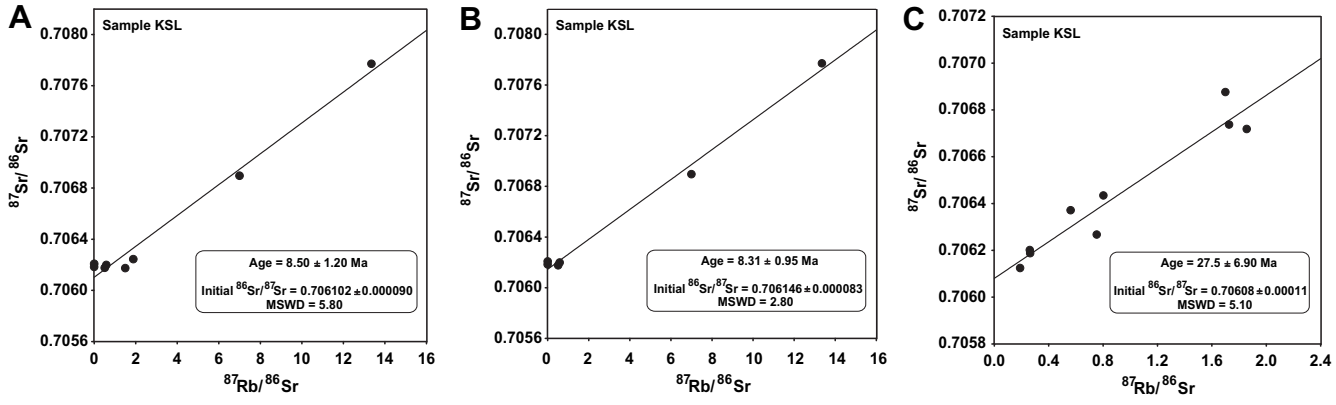

Fig. 5. Rb–Sr isochron diagrams for location KSL (A) The 0.1–0.2 μm fraction of two untreated sub-samples and leachate-residue-untreated fractions from the <0.1 μm size. (B) The leachate-residue-untreated fractions from the <0.1 μm size; (C) The leachate-residue-untreated fractions from 2 to 1, 4 to 2 and >4 μm sizes.

with their REE patterns (Uysal et al., 2006) pointing to the involvement of metamorphic fluids or interaction of such fluids with crustal parent rocks (subduction–accretion complexes) containing some mantle components.

6.2. Significance of the Rb–Sr geochronology

According to Şengör (1979) and Şengör et al. (2005), the generation of the NAFZ was a result of the westward movement of the Anatolian block away from the Arabian–Anatolian collision zone. A more recent alternative hypothesis suggests that the westward translation of Turkey is related to the Hellenic slab subduction, which started earlier than the Miocene Arabia-Eurasia collision (Okay et al., 2008). Although our previous K–Ar data and current Rb–Sr isochron results indicate that there have been continuous fault movements along the Neotethyan orogenic suture zone since the Late Paleocene, drawing a conclusion on the origin of the NAFZ is beyond the scope of the this study. Our current Rb–Sr isochron results for the illitic clays in KSL location are consistent with the Middle Miocene age of the NAFZ (8–10 Ma) that was suggested by Şengör (1979), Westaway (2003) and Şengör et al. (2005). However, older ages obtained from Rb–Sr isochron for the illite–smectite in KHS location and previous K–Ar results for fault gouge illites from the middle part of the NAFZ (see Uysal et al., 2006) may also be interpreted as supporting evidence for the hypothesis by Okay et al. (2008). If the model of Şengör et al. (2005) is correct, then the older ages must reflect earlier fault activities that occurred along the orogenic suture zone, unrelated to the actual NAFZ that was developed along the course of the pre-existing faults.

7. Conclusion

The authigenic illite–smectites of fault gouge samples from the North Anatolian Fault Zone are entirely free from detrital 2 M illite and thus suitable for dating of syntectonic clay precipitation. The Rb–Sr data arrays of leachate, residue and untreated aliquots prepared from various size fractions of samples revealed statistically meaningful ages ranging from 35.6 to 8.3 Ma. The oldest ages are believed to have juxtaposed with the Neotethyan orogenic suture zone. However, the younger age of 8.3 Ma is nearly conformable with our previous K–Ar data and the Middle Miocene age of the NAFZ (8–10 Ma) that was suggested by Şengör (1979), Westaway (2003) and Şengör et al. (2005). The task of fault dating is a challenging work particularly if the gouge material is from a giant fault such as NAFZ where the age of orogenic suture zone may mask the timing of initiation of the latest fault activity.

Acknowledgements

The Scientific and Technical Research Council of Turkey (TUBITAK Project No. 102Y034) and the Australian Research Council (ARC) are greatly acknowledged for financial support. We are grateful for helpful comments and constructive reviews by Ben van der Pluijm, Tom G. Blenkinsop and an anonymous reviewer, which improved our manuscript.

References

Bozkurt, E., 2001. Neotectonics of Turkey – a synthesis. Geodinamica Acta 14, 3–30.
Clauer, N., Chaudhuri, S., 1995. Clays in Crustal Environments. Isotope Dating and Tracing. Springer Verlag, Heidelberg, Berlin, New York, 359 pp.
Clauer, N., Chaudhuri, S., 1999. Isotopic dating of very low-grade metasedimentary and metavolcanic rocks: techniques and methods. In: Frey, M., Robinson, D. (Eds.), Low Grade Metamorphism. Blackwell Science, Cambridge, pp. 202–226.
Clauer, N., Chaudhuri, S., Kralik, M., Bonnotcourtois, C., 1993. Effects of experimental leaching on Rb–Sr and K–Ar isotopic systems and REE contents of diagenetic illite. Chemical Geology 103 (1–4), 1–16.
Gilg, H.A., Frei, R., 1994. Chronology of magmatism and mineralization in the Kassandra Mining Area, Greece – the potentials and limitations of dating hydrothermal Illites. Geochimica Et Cosmochimica Acta 58 (9), 2107–2122.
Grathoff, G.H., Moore, D.M., Hay, R.L., Wemmer, K., 2001. Origin of illite in the lower Paleozoic of the Illinois basin: evidence for brine migrations. Geological Society of America Bulletin 113 (8), 1092–1104.
Grathoff, G.H., Moore, D.M., 1996. Illite polytype quantification using Wildfire calculated X-ray diffraction patterns. Clays and Clay Minerals 44 (6), 835–842.
Haines, S.H., van der Pluijm, B.A., 2008. Clay quantification and Ar–Ar dating of synthetic and natural gouge: application to the Miocene Sierra Mazatan detachment fault, Sonora, Mexico. Journal of Structural Geology 30 (4), 525–538.
Herece, E., Akay, E., 2003. Geological Map along the North Anatolian Fault. The General Directorate of Mineral Research and Exploration, Ankara, Turkey.
Ludwig, K.R., 2003. User's Manual for Isoplot 3.00. A Geochronological Toolkit for Microsoft Excel. In: Special Publication, vol. 4a. Berkeley Geochronology Center, Berkeley, California.
McClusky, S.C., Balassanian, S., Barka, A., Ergintav, S., Georgie, I., Gurkan, O., Hamburger, M., Hurst, K., Kahle, H., Kastens, K., Kekelidse, G., King, R., Kotzev, V., Lenk, O., Mahmout, S., Mishin, A., Nadaria, M., Ouzounis, A., Paradisissis, D., Peter, Y., Pirilepin, M., Reilinger, R.E., Şanli, I., Seeger, H., Teableb, A., Toksöz, N., Veis, V., 2000. Global positioning system constraints on plate kinematics and dynamics in the eastern Mediterranean Caucasus. Journal of Geophysical Research 105, 5695–5719.
Okay, A.I., Satir, M., Zattin, M., Cavazza, W., Topuz, G., 2008. An oligocene ductile strike-slip shear zone: the Uludag Massif, northwest Turkey – implications for the westward translation of Anatolia. Geological Society of America Bulletin 120 (7–8), 893–911.
van der Pluijm, B.A., Hall, C.M., Vrolijk, P.J., Pevear, D.R., Covey, M.C., 2001. The dating of shallow faults in the Earth's crust. Nature 412, 172–175.
van der Pluijm, B.A., Vrolijk, P.J., Pevear, D.R., Hall, C.M., Solum, J., 2006. Fault dating in the Canadian rocky mountains evidence for late cretaceous and early eocene orogenic pulses. Geology 34 (10), 837–840.
Şengör, A.M.C., 1979. The north Anatolian transform fault: its age, offset and tectonic significance. Journal of the Geological Society 136, 269–282.
Şengör, A.M.C., Tüysüz, O., Imren, C., Sakınç, M., Eyidogan, H., Görür, N., Le Pichon, X., Rangin, C., 2005. The north Anatolian fault: a new look. Annual Review of Earth and Planetary Sciences 33, 37–112.
Şengör, A.M.C., Yilmaz, Y., 1981. Tethyan evolution of Turkey – a plate tectonic approach. Tectonophysics 75 (3–4), 181–241.
Uysal, I.T., Golding, S.D., Thiede, D.S., 2001. K–Ar and Rb–Sr dating of authigenic illite–smectite in Late Permian coal measures, Queensland, Australia: implication for thermal history. Chemical Geology 171 (3–4), 195–211.
Uysal, I.T., Mutlu, H., Altunel, E., Karabacak, V., Golding, S.D., 2006. Clay mineralogical and isotopic (K–Ar, dO-18, dD) constraints on the evolution of the north Anatolian fault zone, Turkey. Earth and Planetary Science Letters 243 (1–2), 181–194.
Westaway, R., 2003. Kinematics of the middle east and Eastern Mediterranean updated. Turkish Journal of Earth Sciences 12, 5–46.